Journal of High School Science

Using in Silico fragment-based drug design to search for potential inhibitors of HPIV hemagglutinin-neuraminidase

Patel A[1]

Submitted: March 25, 2022, revised: version 1, April 17, 2022, version 2, April 18, 2022
Accepted: April 18, 2022

Abstract

Human parainfluenza viruses are the etiological agents of human parainfluenza, a common childhood respiratory disease. Two key steps required for these viruses to replicate are ingress and egress, both of which are mediated by the human parainfluenza hemagglutinin-neuraminidase. This protein possesses a large central catalytic pocket for binding to neuraminic acids located on the host cell surface; this catalytic pocket is a promising target for pharmaceuticals aimed to treat parainfluenza. This paper details the use of fragment-based drug design methods to yield compounds that could potentially competitively inhibit the human parainfluenza hemagglutinin-neuraminidase and prevent the virus from entering or exiting a host cell. Analysis of the compounds identified from the screen indicates that π-effects, primarily π-alkyl and π-ion interactions, could be important factors to consider when designing non-Neu5Ac2en-based scaffolds as human parainfluenza treatments.

Keywords

Fragment-based drug design, AutoGrow4, Human Parainfluenza, Hemagglutinin-Neuraminidase, π-effects

[1]Corresponding author: Ayush Patel, Irvington High School, 41800 Blacow Rd, Fremont, CA 94538, payush2005@gmail.com

Introduction

Human parainfluenza is a respiratory disease that is caused by human parainfluenza viruses (HPIVs). These viruses are members of the family *Paramyxoviridae* that are classified under two viral genera: *Respirovirus* (HPIV-1 and HPIV-3) and *Rubulavirus* (HPIV-2 and HPIV-4) (1). They are a common cause of respiratory illness in children: parainfluenza is the second-most common cause of hospitalization due to lower respiratory tract infection in children under five years of age, falling only behind the related respiratory syncytial virus (RSV) (2,3). Despite this, no vaccine, antibody, or small molecule treatment currently exists that is FDA-approved specifically to inhibit HPIV replication. All existing treatments focus solely on relieving the symptoms of the disease (4).

Like all paramyxoviruses, HPIVs possess a negative-sense, single-stranded RNA (-ssRNA) genome. The HPIV genome is unfragmented and exists within the viral capsid complexed with viral proteins into a single ribonucleoprotein. This genome is approximately 15 kilobases long and encodes six structural proteins. One of these structural proteins is a hemagglutinin-neuraminidase (HPIV-HN) that forms a homotetramer on the viral surface that serves the purpose of mediating the passage of viral particles into and out of the cell (1). HPIV-HN is a membrane-spanning protein that possesses a short 31-residue intraviral domain, a 21-residue transmembrane α-helix, and a large 520-residue ectodomain (5). The HPIV-HN ectodomain also contains the protein's catalytic domain (Figure 1), and it is arranged as a six-bladed β-propellor in which six β-sheets (blades) are arranged in a circular fashion around a central, T-shaped catalytic pocket. This catalytic site is the binding site for neuraminic acid, a carbohydrate located on the cell surface that plays a critical role in viral entry (1).

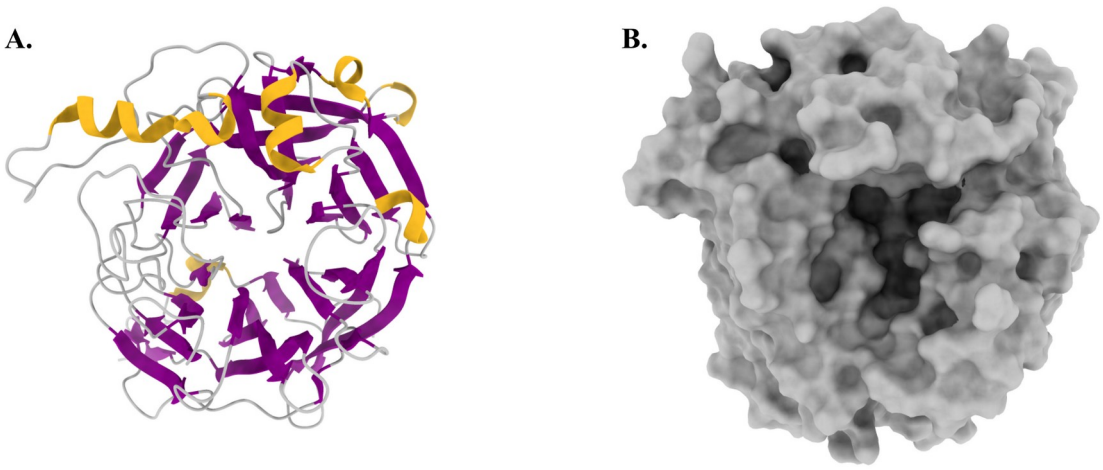

Figure 1: Cartoon and molecular surface representations of the HPIV-HN catalytic domain (PDB ID: 4XJQ) (3). This domain possesses a 6-bladed β-propellor surrounding a large central catalytic pocket.

Ingress of HPIV requires HPIV-HN to bind to the aforementioned neuraminic acids; this process subsequently regulates membrane fusion between virus and cell (1). In mature virions, HPIV-HN interacts with and stabilizes the fusion (HPIV-F) protein in a metastable, spring-loaded conformation. However, upon binding to neuraminic acid residues, HPIV-HN permits HPIV-F to undergo a drastic conformational change that leads to the fusion of the viral membrane with the host cell membrane. The inner contents of the virus are then emptied into the host where they will replicate to yield new viruses. The mechanism that underlies the interaction between HPIV-HN and HPIV-F is as of now still unknown (6). However, current data suggests that this interaction is mediated by the HPIV-HN stalk region and could occur either by dissociation of the head domains (which appears to be the more likely mechanism) or by a conformational change propagated through the stalk upon binding (7).

HPIV-HN is also necessary during viral budding, during which the protein releases mature virions *via* its neuraminidase activity. Dirr, et al. (2015) found evidence that the HPIV-3 HN uses a general mechanism similar to other known neuraminidases, such as the influenza NA protein (3). In this mechanism, HPIV-HN cleaves neuraminic acids from their respective glycans *via* a conserved tyrosine residue (Tyr530 in HPIV-HN) located in the catalytic site (3). The hydroxyl group of this tyrosine acts as a nucleophile that attacks C_2 of the bound neuraminic acid. This process dissociates the neuraminic acid from the rest of the glycan and results in an intermediate in which the neuraminic acid is covalently linked to the catalytic tyrosine residue. This covalent bond is broken by a hydrolysis reaction, which yields a free neuraminic acid and a functioning HPIV-HN (8).

Current efforts to design inhibitors of HPIV-HN revolve around substitutions made on an analog of the intermediate compound in the neuraminidase reaction, Neu5Ac2en (9). Compounds such as zanamivir (Relenza®, FDA-approved to treat illness caused by influenza) and BCX-2798 were identified as potential inhibitors of HPIV-HN using this technique (10,11). These inhibitors are intended to act in one of two ways: they can either competitively inhibit HPIV-HN binding to neuraminic acid or block the HPIV-HN neuraminidase mechanism. An investigation into the binding orientations of each of N-acetylneuraminic acid (Neu5Ac), Neu5Ac2en, and zanamivir with HPIV-HN (PDB IDs: 1V3C, 1V3D, 1V3E) revealed that Neu5Ac2en-based inhibitors and related compounds appear to bind to HPIV-HN through an extensive network of water-mediated hydrogen bonds (Figure 2) (12). These types of hydrogen bonds form when a water molecule is placed such that it forms hydrogen bonds between a ligand and the target protein simultaneously, linking them together. In addition to this, Neu5Ac2en-based inhibitors also form several conventional hydrogen bonds (direct protein-ligand hydrogen bonds), salt bridges (hydrogen bonds compounded with an ionic interaction), and London dispersion forces with HPIV-HN.

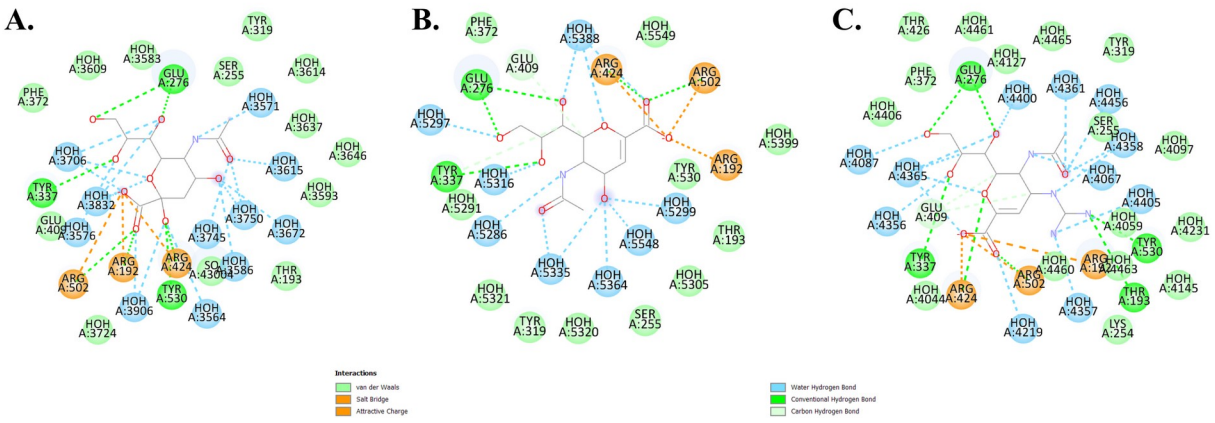

Figure 2: Structures and key molecular interactions of (A) Neu5Ac, (B) Neu5Ac2en, and (C) zanamivir (PDB IDs: 1V3C, 1V3D, 1V3E) (12). Water-mediated and conventional hydrogen bonds, as well as salt bridges, play a major role in stabilizing each ligand to the protein target.

In recent years, major advancements have been made in computer-aided drug design (CADD) that have enabled efficient screening of complex areas of chemical space at a low cost *via* high-throughput virtual screening (HTVS). Specifically, methods such as *in silico* fragment-based drug design (FBDD) using click chemistry have also made it possible to generate extensive libraries of chemically feasible compounds that can subsequently be screened through HTVS (13,14). In this paper, the *in silico* FBDD approach to drug design was used to yield as-of-yet unsynthesized high-affinity inhibitors of HPIV-HN that could later be synthesized and tested *in vitro* for their efficacy against parainfluenza viruses.

Methods

Fragment-Based Drug Design

The library of compounds was synthesized using AutoGrow4, an open-source computer program designed for *in silico* FBDD by Jacob D. Durrant and Jacob O. Spiegel (14). The software uses click chemistry to combine a library of input fragments with assorted molecules into a large library of "mutants" for screening. Each library is called a generation, and each generation is used as an input to yield the next generation. The run was seeded with 6,103 compounds with molecular weights ranging from 100 to 150 daltons. The algorithm was run for two generations to yield several compounds with a high binding affinity for HPIV-HN. The input parameters can be found in the supporting information. All calculations were run on a Dell Latitude E5470 computer with a 4-core Intel i5 processor at 2.60 GHz and 24 GB of RAM.

Docking and Analysis

AutoGrow4 docked all compounds in this study using QVina2 (15). QVina2 is a docking algorithm that combines heuristic techniques with the high reliability of AutoDock Vina (designed and maintained by the Scripps Institute) for faster and more efficient docking. Compounds in each generation were docked to an X-ray diffraction model of HPIV-HN from an HPIV-3 virus (PDB ID: 4XJQ) (3) and ranked by docking score from best to worst. Information regarding specific interactions between each compound and HPIV-HN was extracted using Discovery Studio Visualizer® , a molecular visualization tool developed by Dassault Systèmes (16). Figures of protein-ligand complexes were visualized using UCSF ChimeraX (17), and figures of 2D compound representations were generated using ChemAxon's MarvinSketch (18). ADMET was carried out using pkCSM (19) and similarity searches were carried out using the 3D similarity search function of PubChem (20).

Results and Discussion

The FBDD run yielded 555 compounds with an estimated free energy binding affinity (ΔG) lower than -8 kcal/mol. 57 of those compounds had an estimated binding affinity lower than -9 kcal/mol. All compounds screened in this study were filtered to conform to Lipinski's Rule of 5 for orally bioactive pharmaceuticals (21). Figure 3 provides information regarding the binding orientations and affinities of the top ten hit compounds (each with a ΔG less than -9.5 kcal/mol). Figure 4 is a compilation of the structures of the top hit compounds. For simplicity, the six-number identification sequence provided by AutoGrow4 for each chemical entity is used when referencing inhibitors.

The top ten hit compounds were subjected to a virtual ADMET screen to predict their pharmacokinetics with the assumption that they would be orally administered. All ten compounds were predicted to possess some degree of hepatotoxicity and had low predicted unbound blood fractions, indicating that they were unsuitable for oral delivery. However, both of these issues could potentially be circumvented via intranasal (IN) delivery, in which drugs are administered using a spray directed into the nostrils (22). IN administration circumvents the need for drugs to travel through the blood as such methods deliver the compounds directly to the respiratory system. Furthermore, a search for intranasally-administered drugs on LiverTox revealed a potential correlation between respiratory administration and a lack of hepatotoxicity (23); this correlation is likely due to the fact that respiratory administration reduces the distribution of the drug across the body and is potentially extendable to the compounds identified in this paper. One compound was predicted to exhibit AMES toxicity and four others were predicted to inhibit the function of $K_v11.1$, a subunit of a potassium ion channel critical for normal heart function (24). The remaining five compounds (M516120, M356073, M769741, M629362, and M757703) show promise as respiratory-administered therapeutics for HPIV treatment. A 3D similarity search was carried out on each compound to expand this set, but no similar compounds were identified.

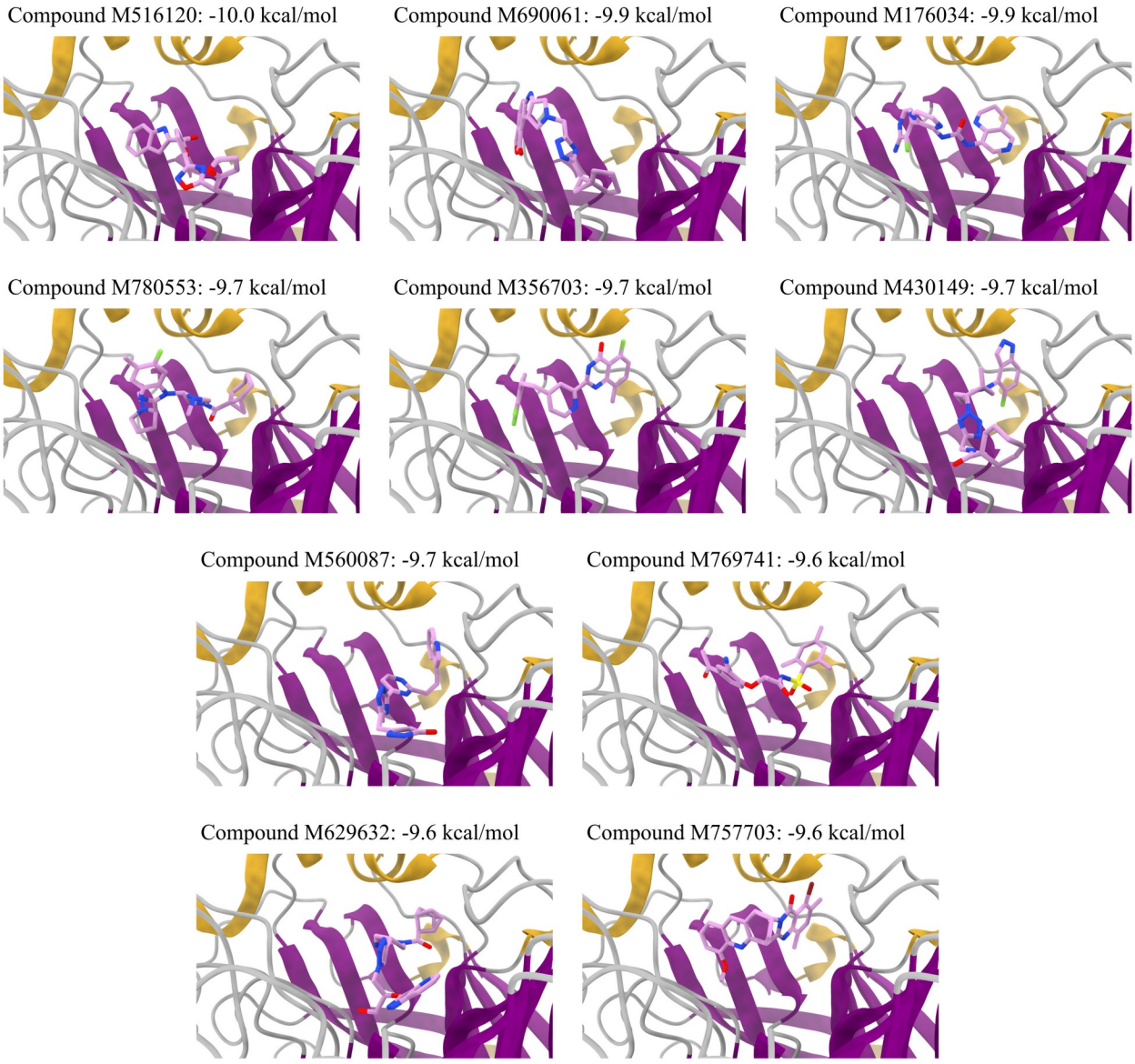

Figure 3: Binding orientations and affinities of the top ten hit compounds identified in this study.

An investigation into the noncovalent interactions between each hit compound and HPIV-HN revealed that π-effects likely play a significant role in the high binding affinities of the identified compounds. The π-effects involved in stabilizing the inhibitors within the binding pocket can be divided into five major groups as defined by Discovery Studio Visualizer: π-alkyl, π-ion, π-sigma, π-sulfur, and π-π interactions. Of these five groups, π-alkyl and π-ion interactions were the most prevalent across the hit compounds and the receptor; each of the other three interactions were only noted in a small number of hits and hence, will not be discussed further. The extent of the effects of these five groups of π-

interactions is a potential subject for future investigation into identifying key features of molecules that bind to HPIV-HN.

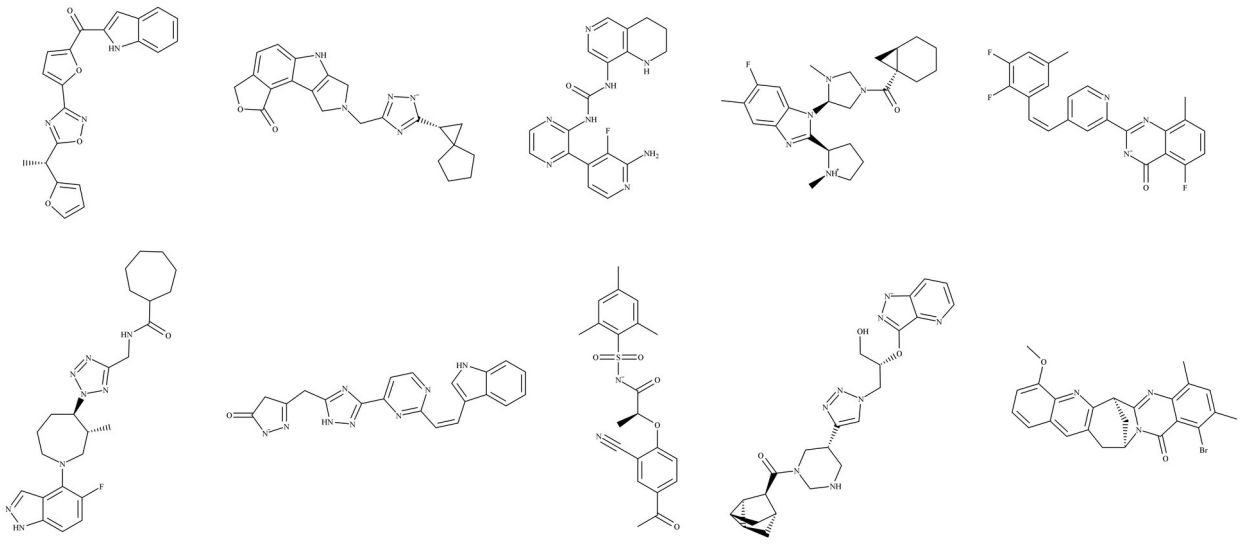

Figure 4: Top ten hit compounds identified in this study. From left to right, they are (first row) M516120, M690061, M176034, M780553, M356073, (second row) M430149, M560087, M769741, M629362, M757703.

π-alkyl interactions were predicted to occur in nine of the ten hit compounds identified in this study; only compound M516120 did not form any π-alkyl interactions with the receptor. These interactions can be further divided into two subgroups. In the first, aromatic rings on the inhibitors interact with alkyl groups of residues within HPIV-HN. The majority of compounds that form π-alkyl interactions with the receptor in this manner possess an aromatic ring moiety that non-covalently binds to either Pro272 or Lys254, two nonpolar residues located adjacent to each other in the binding site. In the second, however, alkyl groups on the inhibitors themselves form π-alkyl interactions with aromatic residues on the protein. This type of π-alkyl interaction is exemplified by the spiro[2.4]heptane moiety of M690061, which interacts with the aromatic phenol R-group of Tyr530.

A further investigation into existing experimental inhibitors of HPIV-HN also provided preliminary evidence that these π-alkyl interactions may play a significant role in improving compound binding affinities. In a 2014 paper, Guillon et al. identified several HPIV-HN inhibitors designed via manipulation of the Neu5Ac2en scaffold (25). Compounds 2 and 5 possessed an alcohol group on C_4. Compounds 7, 8, 9, and 10 had aromatic moieties on C_4. Inhibitors 5, 6, 9, and 10 further differed from the Neu5Ac2en scaffold with the substitution of the C_5 acetamide group

for an isobutyramide group. In both neuraminidase inhibition assays (NI) and hemagglutination inhibition assays (HI), compounds 7, 8, 9, and 10 possessed significantly lower IC_{50} than compounds 2 and 5. Compound 10 (IC_{50} of 2.7μM and 1.5μM in the NI and HI assays, respectively) was identified to form π-alkyl interactions with Val322 through MD simulations (25). It is hypothesized that compounds 7, 8, and 9 also had significantly lower IC_{50} than compounds 2 and 5 for similar reasons, as all of those compounds possess aromatic moieties that could form similar π-alkyl interactions.

π-ion (includes π-cation and π-anion) interactions were the most prevalent class of π-effects noted within the hit compounds; all hits form at least one π-ion interaction with HPIV-HN. This ubiquity can be reasoned by the fact that a large portion of the HPIV-HN binding site is lined with several acidic (Asp216, Glu276, Glu409, Glu549) and basic (Arg192, Arg502) residues. Aromatic moieties within docked ligands preferentially bind to these relatively common residues and form favorable π-ion interactions. The abundance of anionic and cationic side chains within the binding pocket may also explain why aromatic rings were located throughout the catalytic pocket rather than in defined clusters (Figure 5). As a result, scaffolds varying in the positioning of aromatic moieties could, in theory, have similar binding affinities as the hit compounds identified in this study. Experimentation using scaffold-hopping methods *in silico* and *in vitro* is necessary to test this hypothesis.

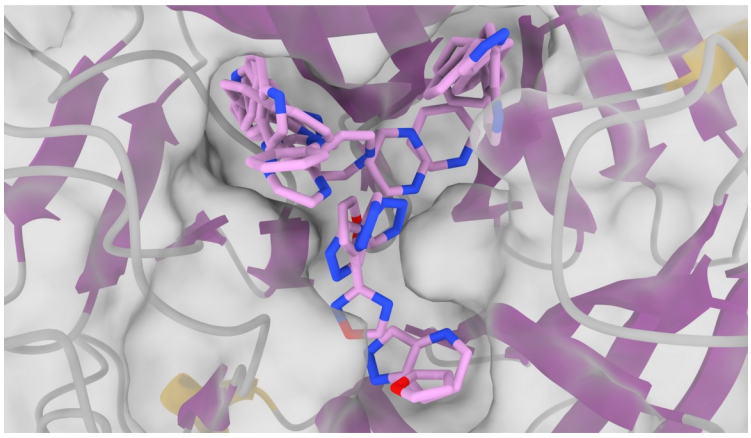

Figure 5: Orientations of the aromatic ring moieties within the top ten hit compounds. As can be seen, rings are positioned throughout the binding site, and there is little clustering.

Limitations

Several drawbacks exist when working with computer programs as a means of screening for compounds of interest. The primary issue lies in the fact that much of the data collected in this investigation (and any investigation that makes use of computer-aided drug design) is based on predictions and estimates made by computer algorithms. Although these

predictions are becoming much more accurate due to advances in *in silico* drug design methodologies, data collected using such methods cannot serve as an absolute replacement for *in vitro* experimentation. In addition, the preparation of the receptor required for the AutoGrow4 run entailed the removal of water molecules and other nonstandard residues in the binding site, which could further reduce the accuracy of docking runs (26). As a result, it is necessary to screen the compounds identified as potential hits *in vitro* to obtain experimental data that supports or refutes these compounds' potencies. In addition to this, crystal structures of each inhibitor complexed with HPIV-HN must be obtained to verify the binding orientation predictions generated in this study.

Conclusions

In conclusion, *in silico* FBDD methods were successfully employed to yield several compounds that could potentially be synthesized and tested for their ability to inhibit HPIV-HN. Analysis of the binding orientations of the top hit compounds identified in this screen indicated that these compounds relied extensively on two primary classes of π-effects; *viz.* π-alkyl and π-ion interactions, for stabilization within the binding pocket,. These interactions present a potential avenue for the development of higher-affinity inhibitors of HPIV infection. Further *in silico* and *in vitro* investigation is required to better understand the implications of these π-effects on the design of HPIV-HN inhibitors.

Abbreviations

CADD: *computer-aided drug design*
FBDD: *fragment-based drug design*
HI: *hemagglutinin inhibition (assay)*
HPIV: *human parainfluenza virus*
HPIV-F: *human parainfluenza fusion protein*
HPIV-HN: *human parainfluenza hemagglutinin-neuraminidase*
HTVS: *high-throughput virtual screening*
IN: *intranasal (administration)*
Neu5Ac: *N-acetylneuraminic acid*
Neu5Ac2en: *2-deoxy-2,3-dehydro-N-acetylneuraminic acid*

Acknowledgments

I would like to thank Ariela Koehler for her assistance throughout this investigation.

Availability of Data and Materials

All data collected in this study, as well as parameters for running AutoGrow4, can be found in the Supporting Information. Please note that the docking processes used in this study are stochastic, and as a result, may vary somewhat between different runs and yield different molecules.

References

1. Henrickson, K. J. Parainfluenza Viruses. *Clinical Microbiology Reviews* **2003**, *16* (2), 242–264.

2. Schmidt, A. C.; Schaap-Nutt, A.; Bartlett, E. J.; Schomacker, H.; Boonyaratanakornkit, J.; Karron, R. A.; Collins, P. L. Progress in the Development of Human Parainfluenza Virus Vaccines. *Expert Review of Respiratory Medicine* **2011**, *5* (4), 515–526.

3. Dirr, L.; El-Deeb, I. M.; Guillon, P.; Carroux, C. J.; Chavas, L. M.; von Itzstein, M. The Catalytic Mechanism of Human Parainfluenza Virus Type 3 Haemagglutinin-Neuraminidase Revealed. *Angewandte Chemie International Edition* **2015**, *54* (10), 2936–2940.

4. Preventing and Treating Human Parainfluenza Viruses (HPIV). www.cdc.gov/parainfluenza/about/prevention-treatment.html (accessed 2022).

5. Hemagglutinin-Neuraminidase. www.uniprot.org/uniprot/P08492 (accessed 2022).

6. Xu, R.; Palmer, S. G.; Porotto, M.; Palermo, L. M.; Niewiesk, S.; Wilson, I. A.; Moscona, A. Interaction Between the Hemagglutinin-Neuraminidase and Fusion Glycoproteins of Human Parainfluenza Virus Type III Regulates Viral Growth in Vivo. *mBio* **2013**, *4* (5).

7. Bose, S.; Zokarkar, A.; Welch, B. D.; Leser, G. P.; Jardetzky, T. S.; Lamb, R. A. Fusion Activation by a Headless Parainfluenza Virus 5 Hemagglutinin-Neuraminidase Stalk Suggests a Modular Mechanism for Triggering. *Proceedings of the National Academy of Sciences* **2012**, *109* (39).

8. Eveno, T.; Dirr, L.; El-Deeb, I. M.; Guillon, P.; von Itzstein, M. Targeting Human Parainfluenza Virus Type-1 Haemagglutinin-Neuraminidase With Mechanism-Based Inhibitors. *Viruses* **2019**, *11* (5), 417.

9. El-Deeb, I. M.; Guillon, P.; Winger, M.; Eveno, T.; Haselhorst, T.; Dyason, J. C.; von Itzstein, M. Exploring Human Parainfluenza Virus Type-1 Hemagglutinin–Neuraminidase as a Target for Inhibitor Discovery. *Journal of Medicinal Chemistry* **2014**, *57* (18), 7613–7623.

10. Greengard, O.; Poltoratskaia, N.; Leikina, E.; Zimmerberg, J.; Moscona, A. The Anti-Influenza Virus Agent 4-Gu-Dana (Zanamivir) Inhibits Cell Fusion Mediated by Human Parainfluenza Virus and Influenza Virus HA. *Journal of Virology* **2000**, *74* (23), 11108–11114.

11. Alymova, I. V.; Portner, A.; Takimoto, T.; Boyd, K. L.; Babu, Y. S.; McCullers, J. A. The Novel Parainfluenza Virus Hemagglutinin-Neuraminidase Inhibitor BCX 2798 Prevents Lethal Synergism Between a Paramyxovirus and Streptococcus Pneumoniae. *Antimicrobial Agents and Chemotherapy* **2005**, *49* (1), 398–405.

12. Lawrence, M. C.; Borg, N. A.; Streltsov, V. A.; Pilling, P. A.; Epa, V. C.; Varghese, J. N.; McKimm-Breschkin, J. L.; Colman, P. M. Structure of the Haemagglutinin-Neuraminidase from Human Parainfluenza Virus Type III. *Journal of Molecular Biology* **2004**, *335* (5), 1343–1357.

13. Konteatis, Z. D. In Silico Fragment-Based Drug Design. *Expert Opinion on Drug Discovery* **2010**, *5* (11), 1047–1065.

14. Spiegel, J. O.; Durrant, J. D. Autogrow4: An Open-Source Genetic Algorithm for De Novo Drug Design and Lead Optimization. *Journal of Cheminformatics* **2020**, *12* (1).

15. Alhossary, A.; Handoko, S. D.; Mu, Y.; Kwoh, C.-K. Fast, Accurate, and Reliable Molecular Docking With QuickVina 2. *Bioinformatics* **2015**, *31* (13), 2214–2216.

16. BIOVIA, Dassault Systèmes, Discovery Studio Visualizer, v21.1.0.20298, San Diego: Dassault Systèmes, 2021.

17. Pettersen, E. F.; Goddard, T. D.; Huang, C. C.; Meng, E. C.; Couch, G. S.; Croll, T. I.; Morris, J. H.; Ferrin, T. E. UCSF ChimeraX: Structure Visualization for Researchers, Educators, and Developers. *Protein Science* **2020**, *30* (1), 70–82.

18. MarvinSketch was used for displaying chemical structures, MarvinSketch version 22.2, ChemAxon (https://www.chemaxon.com).

19. Pires, D. E.; Blundell, T. L.; Ascher, D. B. PKCSM: Predicting Small-Molecule Pharmacokinetic and Toxicity Properties Using Graph-Based Signatures. Journal of Medicinal Chemistry **2015**, 58 (9), 4066–4072.

20. Kim, S.; Chen, J.; Cheng, T.; Gindulyte, A.; He, J.; He, S.; Li, Q.; Shoemaker, B. A.; Thiessen, P. A.; Yu, B.; Zaslavsky, L.; Zhang, J.; Bolton, E. E. PubChem in 2021: New Data Content and Improved Web Interfaces. Nucleic Acids Research **2020**, 49 (D1).

21. Lipinski, C. A.; Lombardo, F.; Dominy, B. W.; Feeney, P. J. Experimental and Computational Approaches to Estimate Solubility and Permeability in Drug Discovery and Development Settings. *Advanced Drug Delivery Reviews* **1997**, *23* (1-3), 3–25.

22. Grassin-Delyle, S.; Buenestado, A.; Naline, E.; Faisy, C.; Blouquit-Laye, S.; Couderc, L.-J.; Le Guen, M.; Fischler, M.; Devillier, P. Intranasal Drug Delivery: An Efficient and Non-Invasive Route for Systemic Administration. Pharmacology & Therapeutics **2012**, 134 (3), 366–379.

23. ncbi.nlm.nih.gov/books/NBK547852/ [2022].

24. Potassium Voltage-Gated Channel Subfamily H Member 2. www.uniprot.org/uniprot/Q12809 (accessed 2022)

25. Guillon, P.; Dirr, L.; El-Deeb, I. M.; Winger, M.; Bailly, B.; Haselhorst, T.; Dyason, J. C.; von Itzstein, M. Structure-Guided Discovery of Potent and Dual-Acting Human Parainfluenza Virus Haemagglutinin–Neuraminidase Inhibitors. *Nature Communications* **2014**, *5* (1).

26. Michel, J.; Tirado-Rives, J.; Jorgensen, W. L. Energetics of Displacing Water Molecules from Protein Binding Sites: Consequences for Ligand Optimization. *Journal of the American Chemical Society* **2009**, *131* (42), 15403–15411.